A. H. STENNING
Professor of Mechanical Engineering.

C. B. MARTIN
National Science Foundation Trainee.

Lehigh University,
Bethlehem, Pa.

An Analytical and Experimental Study of Air-Lift Pump Performance

A one-dimensional analysis of air-lift pump performance in shallow water has been developed which includes the effects of friction and slip between the gas and the liquid. The theory predicts the performance characteristics of these devices successfully, and explains the empirical design rules recommended in earlier publications.

Introduction

Air-lift pumps are frequently used for difficult pumping operations and for underwater exploration, particularly where it is desired to remove sediment from the vicinity of underwater objects without endangering fragile specimens which might be sucked into the intake pipe and damaged by a conventional pump impeller [1].[1]

Fig. 1 shows a schematic of an air-lift pump. Air is injected at the bottom of the pump, and entrains water with it as it rises through the main pipe. Water can be pumped to a considerable height using this simple device.

Although a great deal of experimental work was done on air-lift pumps earlier in the century, especially for applications involving high lifts and deep submergence [2, 3], little information has been published on the performance of air-lift pumps operating in shallow water and at high pumping rates. Pickert [4] presented the results of a set of tests covering a wide range of operating conditions at depths of up to 120 ft. Rennick and Rough [5] have investigated the performance of a model air-lift pump operating with oil in the laminar flow regime.

Analytical studies treated air-lift pumps conceptually as isothermal expansion engines driving water pumps, and multiplied the ideal performance of such a device by an efficiency to account for irreversibilities [6]. The efficiency could lie between 10 and 70 percent. Friction losses were included in some of the theoretical studies [7], but none of the theories considered all of the physical effects in a way which would permit a complete solution. In consequence, it is difficult to use experimental results obtained from one configuration to predict the performance of a different pump.

Fortunately, however, in the past twenty years considerable progress has been made in basic knowledge of two-phase flows, and this information can readily be applied to put the performance prediction of air-lift pumps on a sound analytical footing. This investigation was undertaken with the objective of generating a simple performance prediction method which could be used to calculate the major dimensions and air requirements of air-lift pumps operating in fairly shallow water (up to 30 ft depth). The method can be modified to predict performance at greater depths also, but step-by-step numerical computation is then required to account for the variation in air volume throughout the pump.

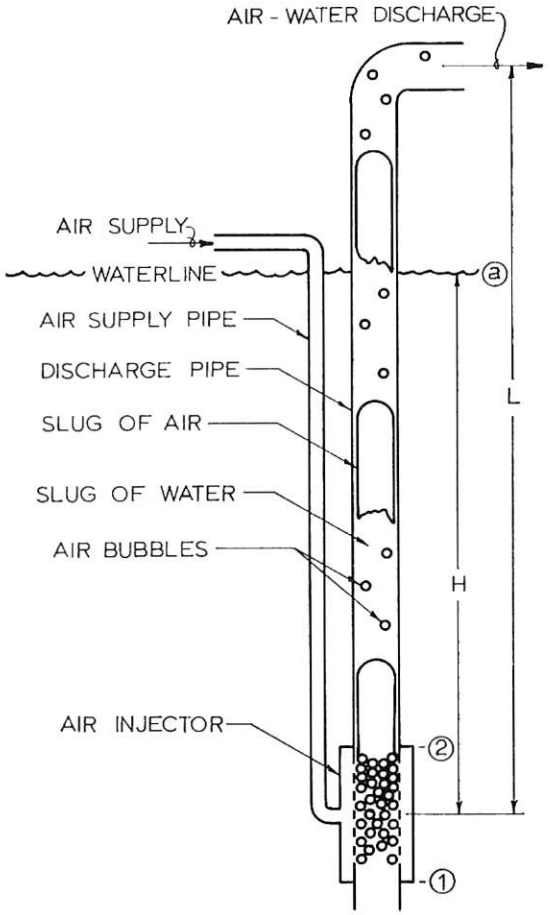

Fig. 1 Schematic of air-lift pump

[1] Numbers in brackets designate References at end of paper.

Contributed by the Fluids Engineering Division and presented at the Winter Annual Meeting, Pittsburgh, Pa., November 12–17, 1967, of The American Society of Mechanical Engineers. Manuscript received at ASME Headquarters, June 14, 1967. Paper No. 67—WA/FE-1.

Nomenclature

A = pipe cross-section area
b = perimeter of pipe
D = pipe diameter
f = friction factor
g = acceleration of gravity
g_c = constant in Newton's second law
H = depth of submergence
K = loss coefficient
L = length of pump
p = pressure
Q = volume flow rate
s = slip ratio
V = velocity
W = weight
ρ = density
τ = wall shear stress

Subscripts

1 = entering pump
2 = leaving injector
a = atmospheric
f = liquid
g = gas

Experiments

A model air-lift pump was built and is illustrated in Fig. 2. The pump was constructed of tubing with a 1.00-in. inside diameter, and had a two ft lucite section near the top for flow visualization. The total height of the pump (defined as L in Fig. 1) was 168 in. A 2-in-dia section with two elbows was added at the top for delivery of the pumped water to a standpipe where the water flow was measured. The air was introduced near the bottom of the pump, through $56^{3}/_{32}$-in-dia holes spaced over a 3-in. length. The air flow rate was measured by a Vol-o-flow flowmeter. Accuracy of the air and water flow rate measurement is estimated as approximately ±2 percent for each quantity. The submergence of the pump (defined as H in Fig. 1) could be varied from zero to 120 in.

Tests were carried out with four values of H/L, of 0.707, 0.629, 0.532 and 0.442. With a fixed value of H, the air flow rate was gradually increased from zero to the maximum available in small steps, and the water flow rate was measured for each value of air flow.

The results of these experiments are displayed in Fig. 3, as water volume flow rate plotted against air volume flow rate evaluated at the mean static pressure in the pump. For each value of H/L, there is an air flow rate which produces a maximum water flow rate. Increasing the air flow rate beyond this point causes a reduction in the water flow rate. At low air flow rates, slug flow was observed in the pump. As the air flow was increased, transition through the various flow regimes to froth flow was observed. In addition to the unsteadiness inherent in two-phase flow, pressure oscillations with a period of several seconds were observed, and the amplitude of these oscillations increased as the flow rate was increased. It is thought that these low frequency oscillations are similar to the natural convection oscillations discussed by Wallis and Heasley [8].

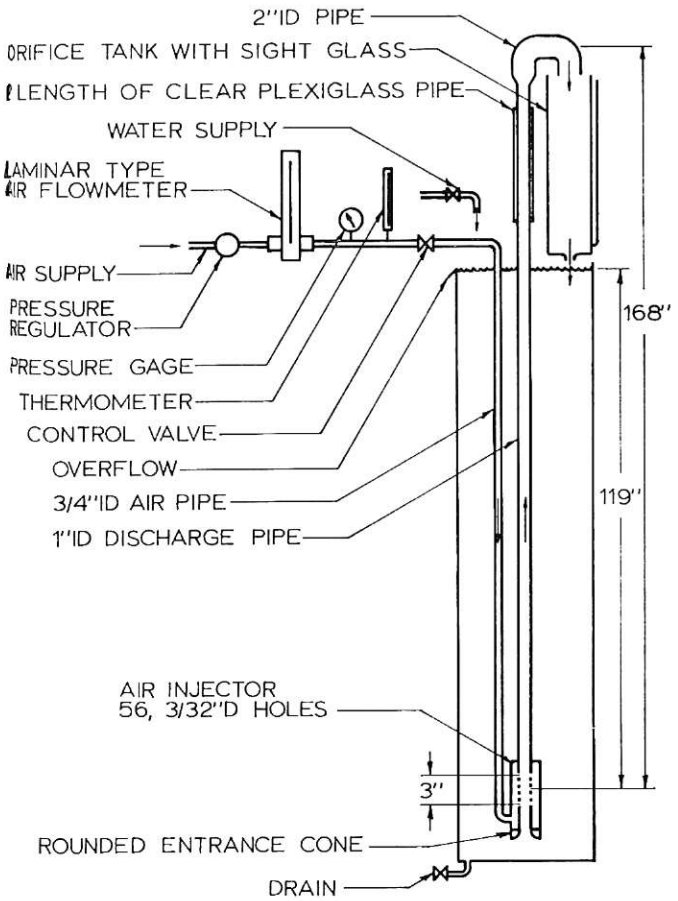

Fig. 2 Arrangement of test apparatus

Analysis

In early publications, air-lift pumps are treated analytically as expansion engines driving water pumps, and an efficiency is used to relate the "air work" to the "pumping work." This efficiency is an extremely variable quantity.

A more profitable approach appears to be to write the continuity and momentum equations, assuming one-dimensional flow in the pump, and to make use of the results of two-phase flow research to solve these equations.

Let us consider the pump shown schematically in Fig. 1. Water enters the bottom of the pump with velocity V_1. Air is injected and mixed with the water, and the mixture leaves the injector with velocity V_2 (assumed the same for both gas and liquid for want of better information). In the riser, some separation occurs between the gas and the liquid, and each component rises with its own average velocity. The slip ratio is defined as $s = \frac{V_g}{V_f}$ where, V_g is the average gas velocity, V_f is the average liquid velocity. Let the static pressure at the pump inlet be P_1. From Bernoulli's equation,

$$P_1 = P_a + \rho_f \frac{g}{g_c} H - \rho_f \frac{V_1^2}{2g_c} \tag{1}$$

where P_a is atmospheric pressure and ρ_f the liquid density.

In the injector, air is injected with the volume flow rate Q_g. Assuming that the mixture velocity leaving the injector is V_2, and neglecting density changes of the air, volume continuity yields

$$\begin{aligned} AV_2 &= Q_g + AV_1 \\ &= Q_g + Q_f \end{aligned} \tag{2}$$

where Q_f = liquid volume flow rate. Hence

$$V_2 = V_1 \left(1 + \frac{Q_g}{Q_f}\right) \tag{3}$$

Writing the continuity equation for the injector, and neglecting the air mass flow rate in comparison with the liquid mass flow rate, we obtain

$$\rho_2 A V_2 = \rho_f A V_1 \tag{4}$$

that is

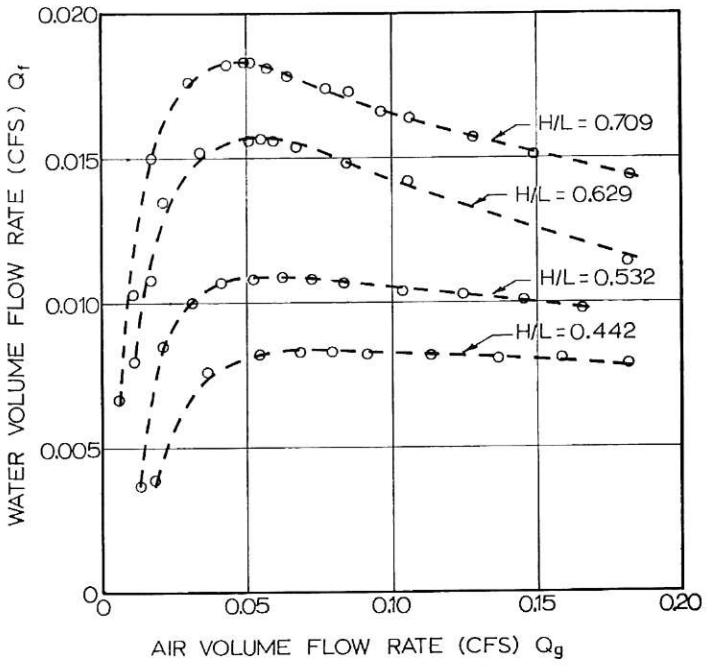

Fig. 3 Performance of model air-lift pump

$$\rho_2 = \rho_f \frac{V_1}{V_2}$$

$$\rho_2 = \frac{\rho_f}{\left(1 + \frac{Q_g}{Q_f}\right)} \tag{5}$$

Applying the momentum equation to the injector as a control volume, we obtain, neglecting wall friction,

$$P_2 = P_1 - \frac{\rho_f V_1}{g_c}(V_2 - V_1) \tag{6}$$

$$= P_1 - \frac{\rho_f V_1 Q_g}{g_c A} \tag{7}$$

Hence, combining equations (1) and (7),

$$P_2 = P_a + \rho_f \frac{g}{g_c} H - \frac{\rho_f V_1^2}{2g_c} - \frac{\rho_f V_1 Q_g}{g_c A} \tag{8}$$

In addition, we can write the momentum equation for the upper portion of the pump. Neglecting momentum changes caused by the flow adjustment after the mixer, the equation becomes

$$P_2 - P_a = \tau \frac{Lb}{A} + \frac{W}{A} \tag{9}$$

where τ is the average wall shear stress, b the wetted perimeter of the pipe, and W the weight of fluid in the pipe.

Griffith and Wallis [9] suggest, for slug flow, the following expression for τ.

$$\tau = f.\ \frac{\rho_f}{2g_c}\left[\left(\frac{Q_f}{A}\right)\right]^2\left[1 + \frac{Q_g}{Q_f}\right] \tag{10}$$

where f is the friction factor, to be obtained assuming that water alone flows through the pipe, with a volume flow rate of $(Q_f + Q_g)$. Equation (10) is, in fact, identical in form with that obtained if the mixture is regarded as homogeneous and the wall stress equated to $f\frac{\rho_2 V_2^2}{2g_c}$.

The weight of the fluid in the pipe is equal to the weight of the liquid plus the weight of the gas.

$$W = \frac{Lg}{g_c}(\rho_f A_f + \rho_g A_g) \tag{11}$$

where A_f is the flow area for the liquid, A_g the flow area for the gas, and ρ_g the density of the gas. Also,

$$Q_f = A_f V_f = A V_1 \tag{12}$$

$$Q_g = A_g V_g \tag{13}$$

$$A_f + A_g = A \tag{14}$$

Substituting (12), (13), and (14) in (11) and neglecting ρ_g in comparison with ρ_f we obtain

$$W = \frac{Lg}{g_c} \frac{\rho_f A}{\left[1 + \frac{Q_g}{sQ_f}\right]} \tag{15}$$

where

$$s = \frac{V_g}{V_f}$$

Substituting (10) and (15) in (9) we find

$$P_2 = P_a + \frac{4fL}{D}\frac{(\rho_f V_1^2)}{2g_c}\left[1 + \frac{Q_g}{Q_f}\right] + \rho_f \frac{g}{g_c} \frac{L}{\left[1 + \frac{Q_g}{sQ_f}\right]} \tag{16}$$

Equating (8) and (16), after some rearrangement the following equation is obtained:

$$\frac{H}{L} - \frac{1}{\left[1 + \frac{Q_g}{sQ_f}\right]} = \frac{V_1^2}{2gL}\left[(K+1) + (K+2)\frac{Q_g}{Q_f}\right] \tag{17}$$

where $K = \frac{4fL}{D}$, and D is the hydraulic diameter of the pipe. Sudden expansion losses, elbows, etc., can be accounted for by increasing the effective value of K. For slug flow, Griffith [10] presents the following expression which may be used to find s:

$$s = \frac{V_g}{V_f} = 1.2 + 0.2\frac{Q_g}{Q_f} + \frac{0.35\sqrt{gD}}{V_1} \tag{18}$$

For the range of flows and pipe diameters which yield the best performance, s is normally between 1.5 and 2.5. Q_g in equations (17) and (18) should be evaluated at the average pressure in the pump.

In Fig. 4, the relationship given by equation (17) is plotted as $\frac{V_1}{\sqrt{2gL}}$ against $\frac{Q_g}{Q_f}$, that is against $\frac{Q_g}{AV_1}$, for $H/L = 0.7$, $K = 5$, and values of s equal to 1.5 and 2.0. It can be seen that a maximum value of V_1 (that is of water flow rate) occurs as Q_g is increased, and that beyond this maximum an increase in air flow reduces the liquid pumping rate. The performance is not very sensitive to changes in slip ratio, the maximum flow rate increasing by only 12 percent when s is decreased from 2.0 to 1.5. Physically, the maximum water flow rate occurs when the frictional pressure drop caused by further addition of air exceeds the buoyancy effect of the additional air.

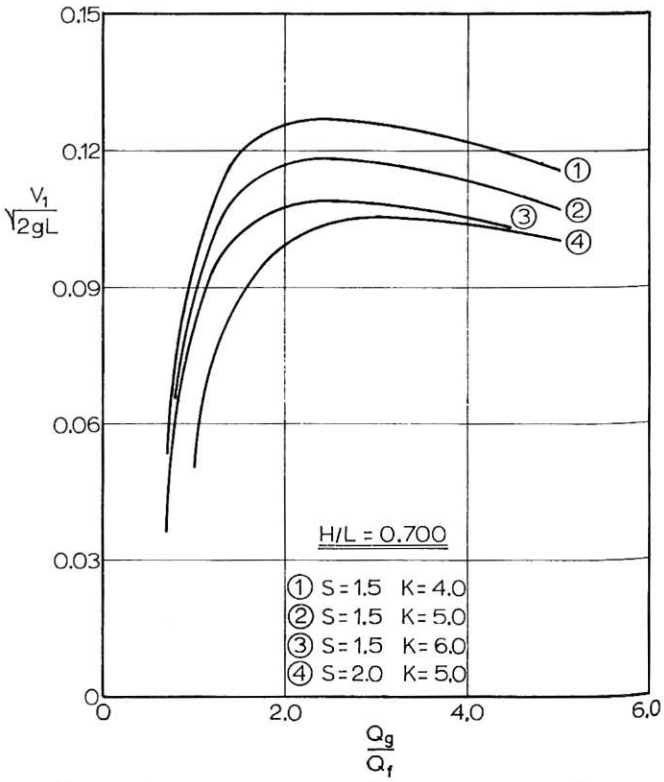

Fig. 4 Theoretical performance with constant s, constant K

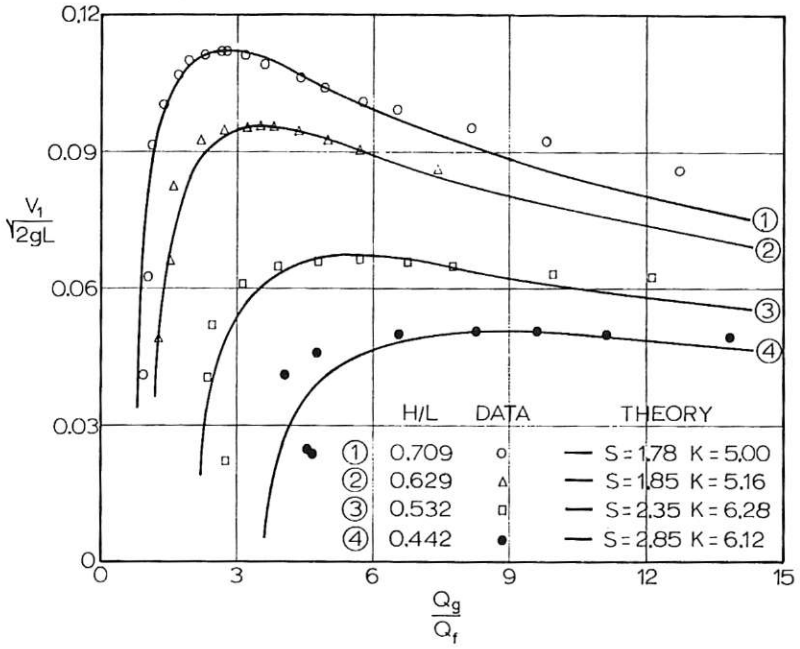

Fig. 5 Comparison of theoretical performance with experimental values

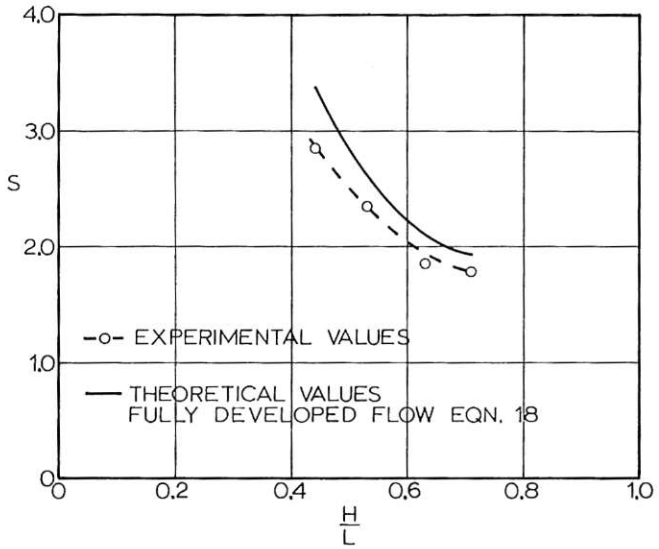

Fig. 6 Variation of slip ratio with $^{H}/_{L}$

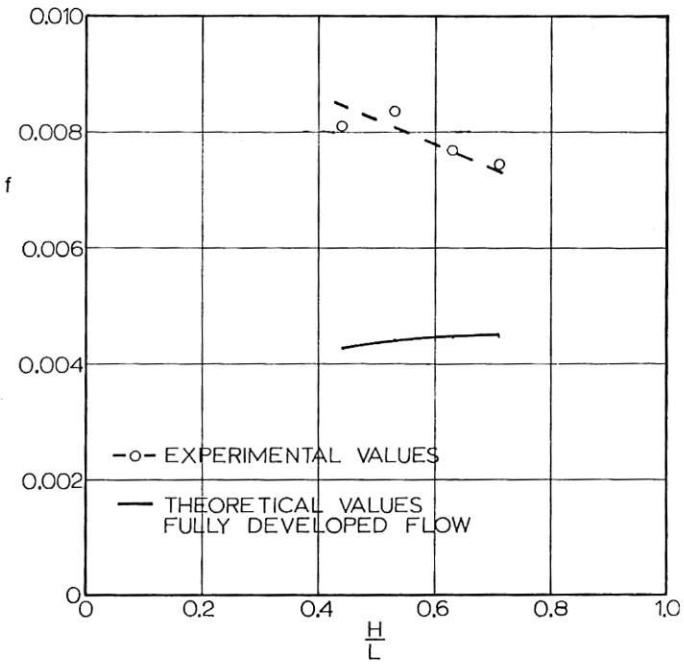

Fig. 7 Variation of effective friction factor with $^{H}/_{L}$

In Fig. 4, the effect of K on performance is also shown. $\frac{V_1}{\sqrt{2gL}}$ is plotted against $\frac{Q_g}{AV_1}$ for $^{H}/_{L} = 0.7$, $s = 1.5$, and $K = 4$, 5, and 6. A 20 percent increase in K produces a 9 percent reduction in maximum pumping capacity.

Comparison of Theory and Experiment

Although s and K will not remain constant over the flow range of a pump, the predicted performance is sufficiently insensitive to small changes in these parameters to suggest that it might be possible to represent the behavior of a pump with fixed $^{H}/_{L}$ fairly well using constant values for s and K.

The performance data obtained experimentally were therefore recalculated in the form suggested by the analysis and values of s and K chosen for each $^{H}/_{L}$ to fit the maximum water flow rate and the corresponding air flow rate. The experimental points, together with the corresponding theoretical curves, are plotted in Fig. 5. The theoretical curves with s and K fitted at the peak match the experimental results over a wide range of flows within 10 percent, and are within 5 percent for the larger values of $^{H}/_{L}$.

The fitted value of s is plotted against $^{H}/_{L}$ in Fig. 6, together with the values predicted by equation (18) at the peaks. Agreement is quite good over the whole range of $^{H}/_{L}$, although the experimental values are smaller than the theoretical values.

After subtracting the (small) elbow losses from the fitted values of K, an effective friction factor was calculated and is plotted against $^{H}/_{L}$ in Fig. 7. The friction factor is considerably larger than the value of approximately 0.0045 which would be predicted using the method recommended by Griffith and Wallis for fully developed flow, but since entrance effects can persist for several hundred diameters in two-phase flow [11], the discrepancy is not too surprising.

The reasons for the rules of thumb suggested in the older publications now become apparent. It is frequently mentioned that

H/L should not fall below about 0.6, and indeed it can be seen from Fig. 5 that a substantial reduction in output does occur for smaller values of H/L. Also, the optimum ratios for $\frac{Q_g}{Q_f}$ are said to lie between 1 and 2, and this is also confirmed by the present theory and experiments.

Preliminary Design Example

For preliminary design purposes it is suggested that the value of s should be obtained from Fig. 6 using the design value of H/L, and that a value for f of 0.008 should be used. The pumping rate can then be calculated as a function of air flow for several different pipe diameters, and the best pipe diameter selected. In general, increasing the pipe diameter decreases the air flow requirement for a given pumping rate, but the size and weight of the piping will also be important factors, especially in marine installations.

Calculations of the performance of a pump with a 4-in-dia pipe, $H = 30$ ft, $L = 40$ ft, have been made using the above method and the results are presented in Fig. 8 as water flow rate plotted against air flow rate, both in cfm with the air volume flow rate adjusted to atmospheric pressure. A peak water output of 34 cfm is predicted. Marks's handbook [12] suggests that the maximum economical pumping rate for a 4-in. pipe is 22 cfm, and it can be seen from Fig. 8 that the air flow does increase rapidly above 22 cfm water flow rate.

Conclusions

It appears that the one-dimensional theory forms a good basis for the performance analysis of air-lift pumps. Additional data are needed for effective slip ratios and friction factors of larger pumps. The analytical method can be extended to handle greater depths of submergence by breaking the total pipe length up into pieces for which the air density can be considered approximately constant for calculation purposes.

Acknowledgment

The authors are grateful to Professor H. P. Frohlich of the University of Miami for drawing their attention to the lack of basic knowledge of air-lift pump performance.

References

1 DeViney, C. A., "Air Lifts," *Compressed Air*, April 1967.

2 Ward, C. N., "Experimental Study of Air Lift Pumps and Application of Results to Design," *Bulletin of the University of Wisconsin*, Serial No. 1265, Engineering Series, Vol. 9, No. 4, 1924.

3 Purchas, A. W., "Some Notes on Air-Lift Pumping," *Trans. I. Mech. E.*, Nov. 1917, pp. 613–697.

4 Pickert, F., "The Theory of the Air-Lift Pump," *Engineering*, Vol. 34, 1932, p. 19–20.

5 Rennick, G. E., and Rough, R. L., "Vertical Flow of Oil and Gas Mixtures in Small-Diameter Siphon-Type Flowstrings," United States Bureau of Mines RI6670, 1965.

6 Ivens, E. M., *Pumping by Compressed Air*, Wiley, New York, 1920.

7 Stepanoff, A. J., "Thermodynamic Theory of the Air Lift," TRANS. ASME, Vol. 51, 1929, pp. 49–55.

8 Wallis, G. B., and Heasley, J. H., "Oscillations in Two-Phase Flow Systems," *Journal of Heat Transfer*, TRANS. ASME, Series C, Vol. 83, No. 3, Aug. 1961, pp. 363–369.

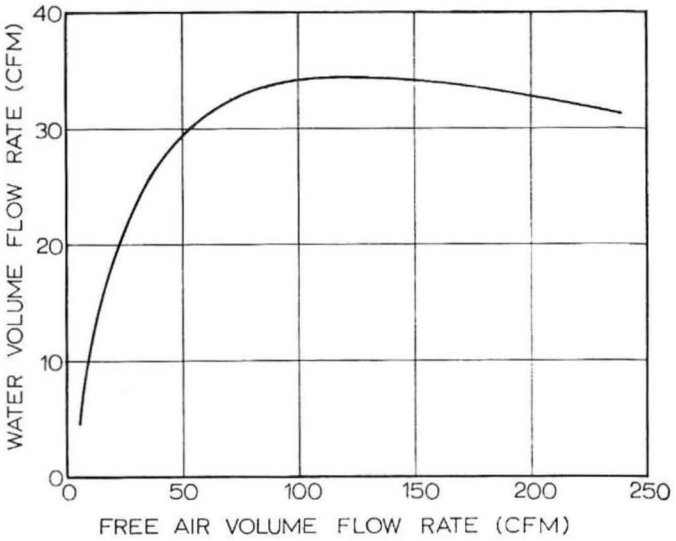

Fig. 8 Predicted performance of 4-in-dia air-lift pump. $H = 30$ ft, $L = 40$ ft.

9 Griffith, P., and Wallis, G. B., "Two-Phase Slug Flow," *Journal of Heat Transfer*, TRANS. ASME, Series C, Vol. 83, No. 3, Aug. 1961, pp. 307–320.

10 Griffith, P., "The Prediction of Low-Quality Boiling Voids," *Journal of Heat Transfer*, TRANS. ASME, Series C, Vol. 86, No. 3, Aug. 1964, pp. 327–333.

11 Moissis, R., and Griffith, P., "Entrance Effects in a Two-Phase Slug Flow," *Journal of Heat Transfer*, TRANS. ASME, Series C, Vol. 84, No. 1, Feb. 1962, pp. 29–39.

12 Marks, L. S., *Mechanical Engineers Handbook*, 5th ed., McGraw-Hill, 1951, pp. 1834–1835.